



HAL
open science

Pyrazolo[1,5-a][1,3,5]triazin-2-thioxo-4-ones derivatives as thymidine phosphorylase inhibitors: Structure, drug-like calculations and quantitative structure-activity relationships (QSAR) modeling

Marwa Manachou, Zied Gouid, Zineb Almi, Salah Belaidi, Salima Boughdiri, Majdi Hochlaf

► To cite this version:

Marwa Manachou, Zied Gouid, Zineb Almi, Salah Belaidi, Salima Boughdiri, et al.. Pyrazolo[1,5-a][1,3,5]triazin-2-thioxo-4-ones derivatives as thymidine phosphorylase inhibitors: Structure, drug-like calculations and quantitative structure-activity relationships (QSAR) modeling. *Journal of Molecular Structure*, 2020, 1199, 22p. 10.1016/j.molstruc.2019.127027 . hal-02974009

HAL Id: hal-02974009

<https://hal.science/hal-02974009v1>

Submitted on 9 Jun 2021

HAL is a multi-disciplinary open access archive for the deposit and dissemination of scientific research documents, whether they are published or not. The documents may come from teaching and research institutions in France or abroad, or from public or private research centers.

L'archive ouverte pluridisciplinaire **HAL**, est destinée au dépôt et à la diffusion de documents scientifiques de niveau recherche, publiés ou non, émanant des établissements d'enseignement et de recherche français ou étrangers, des laboratoires publics ou privés.

Pyrazolo[1,5-a][1,3,5]triazin-2-thioxo-4-ones derivatives as thymidine phosphorylase inhibitors: structure, drug-like calculations and quantitative structure-activity relationships (QSAR) modeling

Marwa Manachou,^a Zied Gouid,^{a,b} Zineb Almi,^c Salah Belaidi,^c Salima Boughdiri,^a Majdi Hochlaf^{b,*}

^a Laboratoire de caractérisations, applications et modélisations des matériaux. Faculté des Sciences de Tunis, Université Tunis El Manar, 2092-Tunis, Tunisia.

^b Université Paris-Est, Laboratoire Modélisation et Simulation Multi Echelle, MSME UMR 8208 CNRS, 5 bd Descartes, 77454 Marne-la-Vallée, France.

^c University of Biskra, Faculty of Sciences, Department of Chemistry, Group of Computational and Pharmaceutical Chemistry, LMCE Laboratory, 07000 Biskra, Algeria.

* Corresponding author:

E-mail address: hochlaf@univ-mlv.fr (M. Hochlaf).

Abstract

After benchmarks on pyrazolo[1,5-a][1,3,5]triazin-2-thioxo-4-ones, we carried out B3LYP density functional theory computations on the structure and vibrational spectroscopy of a series of twenty-one of its derivatives exhibiting various extent of inhibitory activity against thymidine phosphorylase (TP). Then, we performed drug-like calculations, quantitative structure-activity relationship (QSAR) modeling and an evaluation of the physicochemical properties of this series. In order to design the relationships between molecular descriptors and TP inhibition by pyrazolo[1,5-a][1,3,5]triazin-2-thioxo-4-ones derivatives, we used a multiple linear regression (MLR) procedure. A QSAR model is predicted. A further external set of molecules was used for validation where a high correlation between experimental and predicted activity values is noticed.

Keywords: DFT calculations; QSAR; Drug-like; TP inhibitory; MLR; pyrazolo[1,5-a][1,3,5]triazin-2-thioxo-4-ones derivatives.

I. Introduction

Pyrazolo[1,5-a][1,3,5]triazine (Figure 1) is an heterocyclic system. It is recognized as an analog of purine in which the 9-N atom is translocated to position 5 of the bicyclic ring system¹. It is a substituent for purine in the area of nucleoside chemistry and many biologically active agents containing this molecule have been developed². It can be found in various drugs³⁻⁵ and it was used in the development of enzyme inhibitors as therapeutic agents⁶⁻⁸. With appropriate structural modifications, this scaffold can be used to fulfill pharmacophoric requirements in the design stage of drug discovery⁹. With the established approaches to chemical synthesis, libraries of compounds can be generated and evaluated for different biological activities¹⁰⁻¹². Several approaches were developed for its preparation¹³ such as the annulation of the 1,3,5-triazine ring onto a pyrazole scaffold¹, the annulation of the pyrazole ring onto a 1,3,5-triazine scaffold¹⁴, the concurrent formation of both the 1,3,5-triazine and pyrazole ring¹⁵ or syntheses via ring transformation reactions¹⁶.

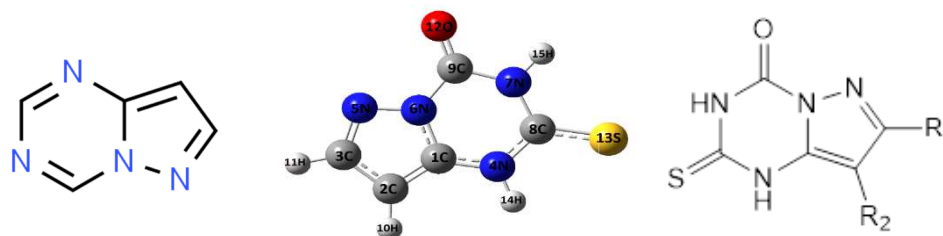


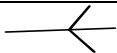
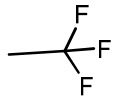
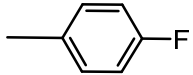

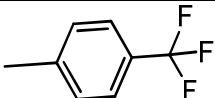
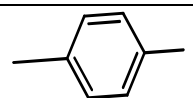
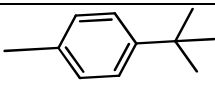
Figure 1: Structures of pyrazolo[1,5-a][1,3,5]triazine (left) and of 1,3-dihydro-pyrazolo [1,5 a][1,3,5] triazin-2-thioxo-4-ones (middle) and of its derivatives (right). See Table 1 for the definition of the R₁ and R₂ groups.

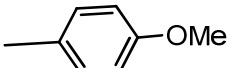
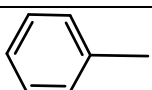
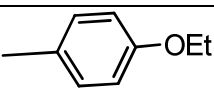
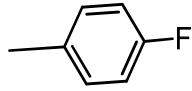
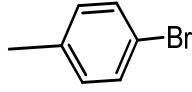
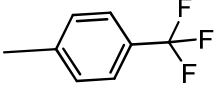
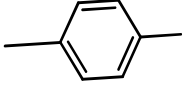
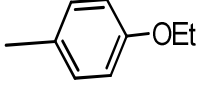
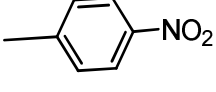
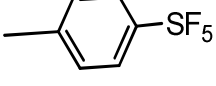
The functionalization of pyrazolo[1,5-a][1,3,5]triazine leads to several compounds with a wide range of applications. Among them, pyrazolo[1,5-a][1,3,5]triazin-2-thioxo-4-ones and its derivatives of interest in the present contribution exhibit a large variety of biological properties and pharmacological applications¹⁷. For instance, DNA gyrase can be selectively inhibited by some pyrazolo[1,5-a][1,3,5]triazines¹⁸. Indeed, it is present in bacteria but not in human, and therefore a good target for antibacterial therapy. Moreover, these heterocyclic cores are active agents to inhibit bronchial inflammation¹⁹ and are useful in the treatment and prevention of central nervous system disorders such as psychosis, schizophrenia, depressions, memory disorders, Parkinson's disease, Alzheimer's disease and Huntington's chorea²⁰. In particular, Pyrazolo[1,5-a][1,3,5]triazin-2-thioxo-4-ones and their derivatives act as anti-tumor agents via the inhibition of thymidine phosphorylase (TP), an enzyme that promotes tumor growth and metastasis and affects the production of 2-deoxy-D-ribose, which in turn suppresses tumor growth²¹. In the literature, we can find several synthesis of these compounds. For instance, Chui and co-workers²² produced several 1,3-dihydro-pyrazolo[1,5-a][1,3,5]triazin-2-thioxo-4-ones derivatives which exhibit various extent of inhibitory activity against TP. Within their synthesis, the pyrazolo[1,5-a][1,3,5] triazine nucleus was constructed using a reaction

that annulated the 1,3,5-triazine ring onto a pyrazole scaffold. Later on, this group ²³ elaborated a fragment-based drug design approach to synthesize, from various substituted 3-aminopyrazoles, a series of 5-chlorouracil-linked-pyrazolo[1,5-a][1,3,5]triazines with TP inhibition activity. Also, Bera et al. ²⁴ obtained nineteen 2-thioxo-pyrazolo[1,5-a][1,3,5]triazin-4-one analogues with mixed TP inhibition endowed with antiangiogenic properties. These authors complemented their investigations by a pharmacological evaluation and a molecular docking study of the discovered series giving insights on the plausible binding sites of these drugs with TP.

The relation between the structure of some pyrazolo[1,5-a][1,3,5] triazine derivatives and their activity was investigated using QSAR approaches. Indeed, El-Shafei et al. ²⁵ developed a QSAR model capable of identifying the key molecular descriptors associated with the biological activity of pyrazolo-diazine and triazine and predicting the cytotoxic effect for other novel pyrazole analogs against EAC cells (Ehrlich Ascites Carcinoma). Also, Zhu et al. ²⁶ elaborated a QSAR model for pyrazolotetrazine derivatives using physicochemical parameters (electronic, Verloop, or hydrophobic) as independent parameters and herbicidal activity as a dependent parameter, where the herbicidal activity correlates best with physicochemical parameters for this set of molecules. It was found that the herbicidal activity is mainly affected by the molar refractivity (MR) and electronic parameters (Hammett's constants).

Table 1: Chemical structures of the molecules under study. See Figure 1.

Compound	R ₁	R ₂
1	H	H
2		H
3		H
4		H
5		H
6		H
7		H
8		H

9		H
10		H
11		H
12	H	Me
13	H	Cl
14	H	Br
15	H	
16	H	
17	H	
18	H	
19	H	
20	H	
21	H	

As said above, Sun et al ²² reported a series of pyrazolo[1,5-a][1,3,5]triazin-2-thioxo-4-ones derivatives as TP inhibitors. They pointed out the effects of various substituents of the pyrazolo[1,5-a][1,3,5]triazin-2-thioxo-4-ones subunit on the TP inhibitory activity. This series of compounds is specified in Figure 1 and Table 1. Their experimental work suggested that the difference in the structure of these molecules could influence their biological activity. Such effects, at the molecular level, are not adequately evaluated yet and they are worth to be investigated using quantum chemical methods.

In the present work, we carried out benchmark studies on the equilibrium geometries, electronic properties and vibrational spectroscopies of pyrazolo[1,5-a][1,3,5]triazin-2-thioxo-4-ones using density functional theory (DFT) and MP2 techniques. These benchmarks revealed that the DFT/B3LYP method is accurate enough to predict the molecular geometries and the electronic

properties and to describe the quantitative structure-activity relationship for the pyrazolo[1,5-a][1,3,5]triazin-2-thioxo-4-ones derivatives compounds with respect to their TP inhibitor activity. In the literature, such validation of the electronic structure method on a subunit to be used for the larger derivatives is done only for some imidazole derivatives²⁷. Then, we characterized the structural and vibrational spectroscopic properties of the series of pyrazolo[1,5-a][1,3,5]triazin-2-thioxo-4-ones derivatives synthesized by Sun et al²². We also performed drug-like calculations, quantitative structure-activity relationship (QSAR) modeling^{27,28} and an evaluation of the physicochemical properties of these compounds. We also deduced various physicochemical and quantum descriptors parameters for modelling their TP inhibitory activity. This model is of great interest for the design of new pyrazolo[1,5-a][1,3,5]triazin-2-thioxo-4-ones derivatives compounds targeting TP inhibitor activity. As explained in Ref. 29, the use of such models avoid the costly and hazardous synthesis of new compounds and the subsequent evaluation of their biological activities.

II. Methodologies

Since there is no experimental structural data available for pyrazolo[1,5-a][1,3,5]triazin-2-thioxo-4-ones, we started our investigations by computing the equilibrium structure and the anharmonic frequencies of pyrazolo[1,5-a][1,3,5] triazin-2-thioxo-4-ones. These benchmarks aim to test the reliability of DFT/B3LYP in predicting the geometry and the properties of our compound (after comparison between methods) in order to be used for the computations of the relatively large pyrazolotriazine derivatives molecular systems. These computations are done using B3LYP³⁰ density functional theory and Møller–Plesset (MP2)³¹ post Hartree-Fock approaches as implemented in GAUSSIAN 09 (version D0.1)³². The atoms were described using the 6-31++G(d,p) or the cc-pVDZ or the aug-cc-pVDZ basis sets^{33,34}. These basis sets are suitable to describe the atoms within the pyrazolo[1,5-a][1,3,5] triazin-2-thioxo-4-ones entities and derivatives. Indeed, they contain polarization functions on heavy atoms and hydrogen, as well as diffuse functions on heavy atoms³³. Also, previous works showed that give good results with respect to the model^{25,27}.

For the pyrazolotriazine derivatives, we carried out full geometry optimizations, in the C₁ point group, followed by harmonic frequencies computations to confirm they correspond to minima (all positive frequencies). We also evaluated their quantum chemical descriptors: dipole moment (DM), energies of frontier orbitals (E_{HOMO} and E_{LUMO}) and electronic energy gaps. We also determined their atomic net charges using the Natural Bond Orbital (NBO) method³⁵. Then, we calculated their physicochemical properties using the QSAR properties module as implemented in HyperChem 8.03 software³⁶. These properties correspond to their molar polarizability (Pol), molar refractivity (MR), partition coefficient octanol/water (logP), molar volume (MV), surface area grid (SAG) and molar weight (MW)³⁷⁻⁴⁰. Also, the calculation of logP quantities is carried out using the atomic parameters as derived by Viswanadhan and coworkers⁴¹. In this work, multiple linear regression analysis (MLR) of molecular descriptors is done using the stepwise strategy in SPSS version 19 for Windows⁴² to

determine statistically a relationship between independent and dependent variables (physicochemical descriptors and biological activities).

III. Benchmarks on pyrazolo[1,5-a][1,3,5]triazin-2-thioxo-4-ones.

a. Equilibrium structure of pyrazolo[1,5-a][1,3,5]triazin-2-thioxo-4-ones

Table 2: Bond lengths (in Å) and valence angles (in degree) of pyrazolo[1,5-a][1,3,5]triazin-2-thioxo-4-ones as computed at different levels of theory. See Figure 1 for the numbering of the atoms.

	DFT/B3LYP		MP2	
	6-31++(d,p)	cc-pVDZ	6-31++(d,p)	cc-pVDZ
C1-N4	1.380	1.379	1.381	1.385
N4-C8	1.370	1.369	1.369	1.371
C8-N7	1.384	1.383	1.389	1.391
N7-C9	1.401	1.401	1.395	1.401
C9-N6	1.404	1.403	1.408	1.413
N6-N5	1.367	1.367	1.361	1.361
N5-C3	1.323	1.324	1.341	1.349
C3-C2	1.424	1.426	1.425	1.425
C2-C1	1.375	1.376	1.380	1.390
C1-N6	1.379	1.378	1.377	1.380
C8-S	1.660	1.665	1.643	1.659
C9-O	1.205	1.204	1.214	1.213
C2-H	1.079	1.083	1.076	1.087
C3-H	1.081	1.086	1.078	1.088
N4-H	1.011	1.011	1.010	1.015
N7-H	1.013	1.013	1.013	1.017
C1-N4-C8	123.5	123.4	123.8	123.4
N7-C9-N6	111.1	111.2	110.6	110.7
C9-N6-N5	123.7	123.8	122.9	122.7
C3-C2-C1	103.4	103.4	103.7	103.5
C1-N6-N5	111.9	112.0	112.6	112.9
N4-C8-N7	113.5	113.7	113.0	113.4

Table 2 lists the main geometrical parameters of the optimized equilibrium geometry of pyrazolo[1,5-a][1,3,5] triazin-2-thioxo-4-ones. These data are obtained using B3LYP and MP2

methods in conjunction with the 6-31G++ (d,p) and the cc-pVDZ basis sets. This table shows that both basis sets lead to similar data. Thus, both basis sets can be used for computations of the structural properties of the pyrazolo[1,5-a][1,3,5] triazin-2-thioxo-4-ones derivatives.

When experimental structures of heterocyclic compounds are not available, MP2 level can be used as reference. Table 2 shows that B3LYP performs quite well since the corresponding geometrical parameters (both bond lengths and angles) are close to those determined by MP2. The deviations between the distances and the angles calculated using B3LYP and MP2 are less than 0.01 Å and less than 1°, respectively. For instance, we calculate a C1-N4 distance of 1.380 Å using B3LYP/6-31++(d,p) which compares well with the MP2/6-31++(d,p) value of 1.381 Å. As for N6-N5 distance, the agreement is satisfactory: its is evaluated 1.367 Å using B3LYP/6-31++(d,p), which is close to the MP2/6-31++(d,p) value of 1.361 Å. These benchmarks prove the reliability of B3LYP to determine the structures for this class of molecules of larger size.

b. Vibrational analysis

The full set of anharmonic frequencies of pyrazolo[1,5-a][1,3,5] triazin-2-thioxo-4-ones is given in Table 3. These data are computed at the MP2/aug-cc-pVDZ and B3LYP/aug-cc-pVDZ levels of theory and using second order perturbation theory (VPT2) approach as implemented in GAUSSIAN. This pyrazolotriazine derivative is a planar molecule. It belongs to the C_s point group. It possesses 27 a' and 12 a'' vibrational modes. Since there is no experimental spectra available for this compound, our data can be used for the assignment of these spectra whenever measured.

The analysis of this table shows that the B3LYP values are close to those obtained by MP2. Indeed, we have less than 20 cm^{-1} differences between both sets of data, except for the C-H stretchings for which differences reach 45 cm^{-1} . Mostly, this vibrational analysis reveals once more the suitability and the reliability of B3LYP for the determination of the vibrational properties of the larger pyrazolo[1,5-a][1,3,5] triazin-2-thioxo-4-ones derivatives.

Table 3: Anharmonic vibrational frequencies (in cm^{-1}) of 1,3-dihydro-pyrazolo [1,5 a][1,3,5] triazin-2-thioxo-4-ones as computed using B3LYP and MP2 in conjunction with the aug-cc-pVDZ basis set. We give also their assignment.

N°	Sym.	MP2	B3LYP	Assignment
1	a'	3459.4	3449.5	N–H stretching
2	a'	3439.1	3423.7	N–H stretching
3	a'	3126.1	3170.9	C–H stretching
4	a'	3107.3	3151.9	C–H stretching
5	a'	1795.6	1789.3	C=O stretching
6	a'	1615.0	1624.6	C=C stretching
7	a'	1505.6	1490.1	C=N stretching

8	a'	1470.1	1463.5	N-H in-plane bending
9	a'	1430.4	1407.9	C-N stretching
10	a'	1379.2	1387.9	C-N in-plane-bending
11	a'	1335.7	1345.3	C-H in-plane-bending
12	a'	1326.6	1305.7	C-N in-plane-bending
13	a'	1262.9	1281.0	C-H in-plane-bending
14	a'	1208.4	1219.6	N-N stretching
15	a'	1162.9	1170.8	C-H in-plane bending
16	a'	1123.5	1120.4	N-H in-plane bending
17	a'	1097.7	1116.3	C=S stretching
18	a'	1028.3	1031.5	C-H in-plane-bending
19	a'	973.5	967.9	C=S stretching
20	a'	912.1	903.0	N-C-C in-plane-bending
21	a'	878.9	856.5	Molecule deformation in-plane-bending
22	a'	772.3	775.2	Molecule deformation in-plane-bending
23	a'	734.4	751.7	N-C-N in-plane-bending
24	a'	726.7	713.4	C-N-C in-plane-bending
25	a'	668.2	655.4	N-C-N in-plane-bending
26	a'	642.1	641.1	Wagging C=O
27	a'	647.1	630.6	Wagging C=S
28	a''	630.9	618.8	C-H out of plane bending
29	a''	611.7	587.3	C-H out of plane bending
30	a''	593.8	605.6	N-C-N out of plane-bending
31	a''	546.2	524.5	N-H out of plane bending
32	a''	506.6	496.5	N-H out of plane bending
33	a''	398.2	401.6	N-N out of plane bending
34	a''	328.8	323.7	N-C-N out-of-plane-bending
35	a''	307.1	303.6	N-H out of plane bending
36	a''	238.9	245.4	C-N out of plane bending
37	a''	151.1	141.1	Rings deformation out-of-plane-bending
38	a''	139.2	133.8	Molecule deformation out-of-plane-bending
39	a''	93.1	90.7	Molecule deformation out-of-plane-bending

c. Natural Bond Orbital (NBO) and Molecular Electrostatic Potential (MESP) surface of pyrazolo[1,5-a][1,3,5]triazin-2-thio-4-ones

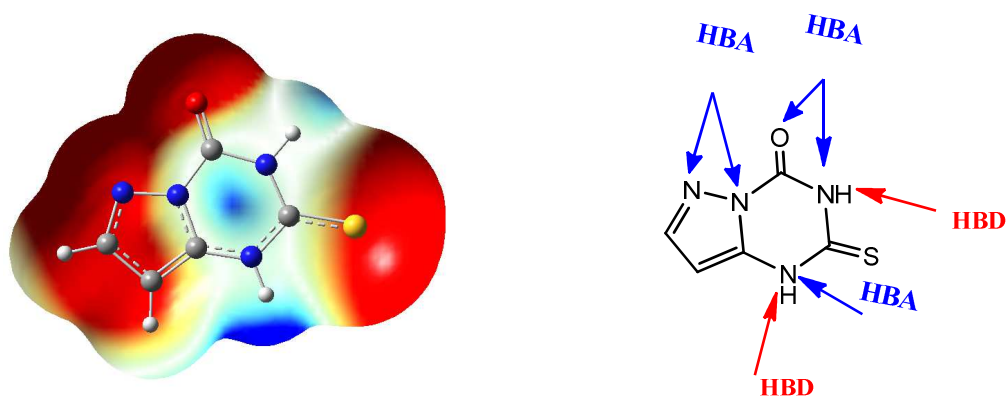


Figure 2: 3D MESP surface map (left) for pyrazolo[1,5-a][1,3,5]triazin-2-thio-4-ones and its hydrogen bond donor (HBD) and hydrogen bond acceptor (HBA) sites (right). The red regions correspond to negative potentials and the blue regions to positive potentials.

The information contained in molecular electrostatic potentials (MESP) has been harnessed for determination of structure, reactivity, electron diffraction and scattering and also the energetics of a wide variety of organic, inorganic, as well as biological molecular systems⁴³. In fact, MESP displays simultaneously the molecular size and shape as well as positive, negative and neutral electrostatic potential regions in terms of the electrostatic surface⁴⁴. Figure 2 shows the MESP surface map of pyrazolo[1,5-a][1,3,5]triazin-2-thio-4-ones. The red color refers to negative potential regions as around the oxygen and sulfur atoms of the pyrazolic cycle. For nitrogens, we compute mostly negative potentials with different magnitudes. These regions are susceptible for electrophilic attacks. Figure 2 shows also that the regions around the hydrogens attached to the nitrogens benzylic cycle are blue (positive potentials). These regions are susceptible for nucleophilic attacks. This analysis agrees with the net charges calculated using natural bond orbital (NBO) model³⁵ (cf. Table 4).

Table 4: B3LYP/6-31++G(d,p) net charges calculated using natural bond orbital (NBO). See Figure 1 for the numbering of the atoms.

Atoms	NBO charges
C ₁	0.353
C ₂	-0.370
C ₃	-0.009
N ₄	-0.602
N ₅	-0.255
N ₆	-0.288
N ₇	-0.662
C ₈	0.224
C ₉	0.839

O ₁₂	-0.550
S ₁₃	-0.135

The present analyses allow identifying the hydrogen bond donor (HBD) and hydrogen bond acceptor (HBA) sites (Figure 2). These characteristics may be helpful for a qualitative understanding of the electrostatic interactions that may take place between reagents or enzyme active sites and the pyrazolo[1,5-a][1,3,5]triazin-2-thioxo-4-ones derivatives under study.

IV. Characterization of the pyrazolo[1,5-a][1,3,5]triazin-2-thioxo-4-ones derivatives

The twenty-one molecules of this series of pyrazolo[1,5-a][1,3,5]triazin-2-thioxo-4-ones derivatives are optimized at the B3LYP/6-31++G(d,p) level of theory. The optimized structures are given in Table S1 of the supplementary material. Close examination of these structures shows that the pyrazolo[1,5-a][1,3,5]triazin-2-thioxo-4-ones part within these compounds has very close structure. Indeed, we compute C=S, C=O, C-C, C-N, N-N and N-H distances of 1.66, 1.20, 1.37, 1.36, 1.01 (all values are in Å), respectively. Thus, the functionalization of this heterocycle slightly disturbs its structure. This is confirmed by the vibrational analysis we performed for this series. Anharmonic frequencies can be obtained after scaling the corresponding harmonic frequencies by the appropriate scaling factor (by 0.9662 for $\omega > 1000 \text{ cm}^{-1}$ and by 0.9833 for $\omega < 1000 \text{ cm}^{-1}$) as discussed in Ref. ⁴⁵. Table 5 presents the respective data for C=S, C=O and both NH elongations. This table shows that similar C=S (of $\sim 1100 \text{ cm}^{-1}$), C=O (of $\sim 1780 \text{ cm}^{-1}$), NH (of $\sim 3500 \text{ cm}^{-1}$) elongations values are computed for all compounds. Indeed, they differ by less than 20 cm^{-1} within the series. Again, this is due to slight perturbation of the heterocycle upon functionalization.

Table 5: Scaled anharmonic vibrational frequencies (in cm^{-1}) (scaling factor 0.9662 ⁴⁵) of some elongation modes of pyrazolo[1,5-a][1,3,5]triazin-2-thioxo-4-ones derivatives as computed using B3LYP/6-31++G(d,p).

	Compounds	C=S	C=O	NH (1)	NH (2)
	1	1086.8	1767.1	3480.7	3498.7
	2	1100.0	1777.7	3497.8	3516.8
	3	1102.0	1791.5	3491.4	3512.8
	4	1102.2	1777.7	3497.0	3516.2
	5	1104.8	1778.3	3496.7	3516.1
	6	1102.9	1780.3	3495.4	3515.2
	7	1098.2	1776.2	3498.2	3516.9
	8	1098.5	1776.1	3498.3	3516.9
	9	1096.4	1774.6	3498.7	3516.8

	10	1101.1	1777.2	3497.6	3516.6
	11	1095.0	1774.4	3498.8	3516.8
	12	1095.4	1780.9	3498.4	3514.6
	13	1092.6	1786.7	3494.1	3501.1
	14	1091.1	1786.2	3493.5	3497.8
	15	1099.4	1782.1	3496.3	3503.2
	16	1099.4	1782.8	3496.5	3502.5
	17	1099.5	1784.3	3495.4	3502.6
	18	1098.9	1780.3	3497.4	3502.2
	19	1097.4	1779.7	3497.6	3502.0
	20	1094.9	1786.0	3493.8	3503.8
	21	1100.2	1785.7	3494.7	3502.6

V. Structure-physical chemistry property relationships

We have studied various physical chemical properties of the series composed by the twenty-one pyrazolo[1,5-a][1,3,5]triazin-2-thioxo-4-ones derivatives. QSAR properties such as van der Waals surface molecular volume ⁴⁶, octanol-water partition coefficient (logP), molar refractivity (MR), polarizability (Pol), solvent-accessible, surface bounded molecular volume and molecular weight (MW) and energies of the HOMO (highest occupied molecular orbital) and LUMO (lowest unoccupied molecular orbital) energies ⁴⁷⁻⁴⁹ are determined. These data are derived using HyperChem and Gaussian softwares and presented in Table 6. We also consider Lipinski rules to identify "drug-like" compounds.

Table 6 shows that the polarizability and molar refractivity are connected to the size and the molecular weight of the studied pyrazolo[1,5-a][1,3,5]triazin-2-thioxo-4-ones derivatives. Indeed, the polarizability and molar refractivity increase when the size and the weight of the compound increases. This result is in agreement with the formula of Lorentz-Lorenz, which gives a relationship between polarizability, the molar refractivity and volume ⁵⁰. For instance, Compound 1 (1,3-Dihydro-pyrazolo[1,5-a][1,3,5]triazin-2-thioxo-4-one) has small values of polarizability (17.32 Å³) and of molar refractivity (34.41 Å³). Whereas Compound 8 (1,3-Dihydro-7-(4-tert-butylphenyl)pyrazolo[1,5-a][1,3,5] triazin-2-thioxo-4-one) has large values of polarizability (34.32 Å³) and of molar refractivity (77.87 Å³).

The presence of the hydrophobic groups in the structure of the pyrazolo[1,5-a][1,3,5]triazin-2-thioxo-4-ones decreases the hydration energy, whereas hydrophilic groups do the opposite (Table 6). The largest hydration energy (17.04 kcal/mol) is computed for Compounds 20 (4-carboxy-3H-1,2,-dithiole-3-thione) and the smaller one (2.45 kcal/mol) is for Compound 10 (1,3-Dihydro-8-(4-nitrophenyl) pyrazolo[1,5-a][1,3,5]triazin- 2-thioxo-4-one). In the biological environment, the polar

molecules are surrounded by water molecules so that Hydrogen bonds can be established between the water molecule and the molecules under study. The donor sites of proton interact with the oxygen atom of water and the acceptor sites of proton interact with water hydrogen atoms. These hydrogen bonds and van der Waals interactions are relatively weak. They are generally reversible in particular between messengers and receivers ⁵¹.

The energies of HOMO and LUMO are related to the reactivity of the molecule. For instance, molecules with electrons at accessible (near-zero) HOMO levels tend to be good nucleophiles because donation of these electrons toward making a new bond is easy. Similarly, molecules with low LUMO energies tend to be good electrophiles because placing an electron into such an orbital is facilitated. Both properties can be connected via the energy gap (ΔE) between the HOMO and the LUMO. Table 6 gives the ΔE values for our derivatives. As can be seen, Compound 20 has the lowest LUMO (-3.299 eV) and the smallest energy gap ($\Delta E = 3.681$ eV). Thus, this compound is the most reactive one.

The lipophilicity is proportional to the hydrophobic character of the substituent's group ⁵². LogP is the most useful parameter for the characterization of the hydrophobicity and the polarity of the compounds. It is an important variable in QSAR studies because the distribution of chemicals between fatty and aqueous phases of a biological system could totally account for the variation in activities. Table 6 reveals that Compound 8 (1,3-Dihydro-7-(4-tert-butylphenyl)pyrazolo[1,5-a][1,3,5] triazin-2-thioxo-4-one) has high value of logP (3.64). This compound generally has a good intestinal absorption owing to a good balance between solubility and passive diffusion permeability ⁵³. In fact, the metabolism is minimized because of the lower binding with metabolic enzymes.

Lipophilic ligand efficiency (LipE) is defined as: $\text{LipE} = \text{pIC}_{50} - \text{logP}$. As a rough guide, medicinal compounds in drug-like space have LipE values in the range 4–7. Table 6 shows that Compound 20 has the highest LipE value (4.05) and it is deemed to be the most optimal compound. For good absorption and permeability, the molecules must satisfy the Lipinski's rule. This rule accounts for molecular properties, which are important for a drug's pharmacokinetics in the human body, including their absorption, distribution, metabolism and excretion. A compound satisfying the Lipinski's rule ⁵⁴ should have $\text{LogP} \leq 5$, a molecular weight (MW) ≤ 500 Da, H-bond donors (HBD) ≤ 5 and H-bond acceptors (HBA) ≤ 10 . If it violates more than one of these parameters, its bioavailability is reduced in addition to a high probability of failure to display drug-likeness. Therefore, our results reveal that the majority of the twenty-one pyrazolo[1,5-a][1,3,5]triazin-2-thioxo-4-ones derivatives satisfy the Lipinski rules. Therefore, we suggest that these compounds do not have any problems with oral bioavailability.

Table 6: Values of chemical descriptors used in the regression analysis. We give the energies of the HOMO (E_{HOMO} , eV) and LUMO (E_{LUMO} , eV), energy gap (ΔE , eV), octanol-water partition coefficient ($\log P$), hydration energy (HE, kcal/mol), polarizability (Pol, \AA^3), molar refractivity (MR, \AA^3), volume (V, \AA^3), surface area (SAG, \AA^2), molar weight (MW, amu). HBA and HBD are the numbers of the hydrogen bond acceptor and donor sites. Nv is for the number of rules violations (not respected). The q values (qC1, qC2, qC3, qN4, qN5, qN6, qN7, qC8, qC9, qO, qS) are the charges on the respective atoms. See text for more details.

Comp.	E_{HOMO}	E_{LUMO}	ΔE	$\log P$	HE	Pol	MR	MV	SAG	MW	LipE	HBA	HBD	Nv	qC1	qC2	qC3	qN4	qN5	qN6	qN7	qC8	qC9	qO	qS
Rules	-	-		< 5	-	-	-	-	-	< 500 $\Delta\alpha$		< 10	< 5	-											
1	-6.789	-1.915	4.874	0.40	-10.42	17.32	34.41	452.51	310.00	168.18	3.76	5	2	0	0.338	-0.349	0.168	-0.584	-0.259	-0.258	-0.644	0.203	0.804	-0.531	-0.151
2	-6.633	-1.799	4.834	1.96	-7.15	24.66	52.74	648.92	410.24	224.29	2.57	5	2	0	0.359	-0.361	0.212	-0.600	-0.273	-0.285	-0.66	0.226	0.838	-0.557	-0.143
3	-7.157	-2.256	4.901	1.21	-9.10	18.89	40.05	533.40	355.52	236.18	3.27	5	2	0	0.362	-0.341	0.069	-0.602	-0.219	-0.275	-0.66	0.218	0.839	-0.539	-0.111
4	-6.665	-1.986	4.679	2.16	-10.18	26.89	59.43	676.66	428.94	286.32	2.21	5	2	0	0.355	-0.337	0.17	-0.602	-0.264	-0.277	-0.661	0.224	0.836	-0.555	-0.134
5	-6.676	-2.063	4.613	2.53	-10.13	28.91	64.01	713.54	448.69	284.77	1.94	5	2	0	0.370	-0.353	0.175	-0.603	-0.262	-0.28	-0.661	0.224	0.835	-0.552	-0.133
6	-6.872	-2.308	4.564	3.02	-11.77	29.61	69.87	726.87	449.37	318.32	1.98	5	2	0	0.356	-0.334	0.165	-0.602	-0.255	-0.276	-0.661	0.222	0.837	-0.551	-0.127
7	-6.476	-1.856	4.620	2.48	-9.28	28.82	64.25	722.08	454.95	264.35	2.23	5	2	0	0.349	-0.328	0.172	-0.601	-0.264	-0.279	-0.661	0.226	0.834	-0.555	-0.141
8	-6.471	-1.850	4.621	3.64	-8.07	34.32	77.87	856.70	520.64	306.44	1.54	5	2	0	0.353	-0.339	0.193	-0.601	-0.266	-0.279	-0.661	0.226	0.836	-0.557	-0.141
9	-6.183	-1.801	4.382	1.76	-12.12	29.46	65.67	744.42	464.76	280.35	2.78	6	2	0	0.338	-0.349	0.167	-0.584	-0.258	-0.258	-0.644	0.203	0.804	-0.531	-0.151
10	-6.603	-1.919	4.684	2.02	-10.49	26.98	59.21	668.00	423.24	250.33	2.31	5	2	0	0.353	-0.335	0.174	-0.601	-0.261	-0.278	-0.661	0.225	0.836	-0.556	-0.138
11	-6.150	-1.787	4.363	2.11	-11.17	31.29	70.42	802.60	497.61	294.38	3.10	6	2	0	0.338	-0.349	0.168	-0.584	-0.259	-0.258	-0.644	0.203	0.804	-0.531	-0.151
12	-6.630	-1.839	4.791	0.86	-9.40	18.61	39.45	506.70	336.01	182.21	3.19	5	2	0	0.352	-0.164	-0.001	-0.601	-0.255	-0.281	-0.662	0.226	0.838	-0.553	-0.143
13	-6.897	-2.090	4.807	0.92	-9.74	19.25	39.22	496.43	332.95	202.63	3.63	5	2	0	0.339	-0.202	-0.011	-0.600	-0.242	-0.277	-0.662	0.220	0.839	-0.546	-0.117
14	-6.871	-2.078	4.793	1.19	-9.69	19.95	42.04	515.21	341.24	247.08	3.16	5	2	0	0.341	-0.281	-0.010	-0.599	-0.242	-0.277	-0.662	0.220	0.839	-0.546	-0.117
15	-6.627	-1.988	4.639	2.37	-11.83	26.89	62.47	673.03	419.30	268.32	2.60	5	2	0	0.371	-0.173	0.009	-0.601	-0.248	-0.282	-0.662	0.224	0.838	-0.551	-0.133
16	-6.626	-2.042	4.584	3.02	-11.77	29.61	69.87	726.87	449.37	329.22	3.18	5	2	0	0.373	-0.175	0.010	-0.601	-0.248	-0.282	-0.662	0.223	0.838	-0.55	-0.130
17	-6.823	-2.234	4.589	3.11	-11.52	28.55	68.22	739.75	457.07	318.32	3.50	5	2	0	0.378	-0.186	0.012	-0.602	-0.245	-0.282	-0.661	0.222	0.838	-0.548	-0.124
18	-6.437	-1.863	4.574	2.70	-10.94	28.82	67.29	716.72	443.16	264.35	3.06	5	2	0	0.370	-0.173	0.009	-0.600	-0.251	-0.282	-0.662	0.226	0.838	-0.553	-0.140
19	-6.222	-1.795	4.427	2.32	-12.83	31.29	73.46	798.23	490.84	294.38	2.48	6	2	0	0.377	-0.176	0.008	-0.601	-0.252	-0.285	-0.662	0.226	0.838	-0.555	-0.142
20	-6.980	-3.299	3.681	2.18	-17.04	28.82	69.57	721.75	446.93	295.32	4.05	8	2	0	0.383	-0.185	0.013	-0.602	-0.242	-0.281	-0.661	0.220	0.838	-0.545	-0.115
21	-6.949	-2.690	4.259	3.50	-12.16	28.08	69.17	790.55	481.39	376.38	3.89	5	2	0	0.381	-0.190	0.012	-0.603	-0.243	-0.281	-0.661	0.220	0.838	-0.546	-0.117

VI. Quantitative structure-activity relationships studies

In order to explain the correlations between the physicochemical/quantum descriptors and the biological activities (IC_{50} values) of the series of the pyrazolo[1,5-a][1,3,5]triazin-2-thioxo-4-ones derivatives, a QSAR study is undertaken to propose a QSAR model. Our QSAR model is selected on the basis of various statistical parameters such as: (i) correlation coefficient (R), which measures the degree of line association between two variables; (ii) square correlation coefficient ($R^2 > 0.6$), which is a relative measure of the fit quality⁵⁵; (iii) standard error of estimate ($SEE < 0.3$) representing absolute measure of the quality of fit (Q); (iv) Fischer's ratio (F), which reflects the ratio of the variance explained by the model and the variance due to the error in the regression. High values of F indicate that the model is statistically significant⁵⁶. The best statistically significant correlations between the biological activity (IC_{50}) and the descriptors are generated after a multiple regression analysis using the software SPSS. They are linked via:

$$\log(1/IC_{50}) = 143.450 + 1.603 \log P - 0.22 \text{ Pol} - 0.046 \text{ MV} + 0,093 \text{ SAG} - 1.232 \text{ E}_{\text{LUOMO}} + 15.734 \text{ qC1} + 4.580 \text{ qC2} + 298.731 \text{ qN4} + 143.115 \text{ qC8} + 30.719 \text{ qS}$$

For the twenty-one compounds of interest, the expression above is obtained with $R = 0.988$; $SEE = 0.196$; $F = 40.79$ and $Q = 5.04$. All the values of the t-statistic are significant, which confirms the significance of each descriptor. Indeed, the square of the correlation coefficient R^2 is equal to 0.976 (> 0.8). This indicates that a good percentage of the total variance in biological activity is accounted for by the model. For SEE, we obtained a low value ($0.196 < 0.3$), which indicates that the statistical fit is accurate. The F-value has found to be statistically significant at 95 % level, since the calculated F value is higher than the tabulated value. The positive value of Q for this QSAR's model suggests its high predictive power and lack of over fitting. In this model, the negative coefficient for the term MV and E_{LUMO} documents that any increase in molecular volume of the compounds causes a decrease in the biological activity. If we want to increase the value of the activity, we can decrease the E_{LUMO} value, for which we suggest the substitution of the pyrazolo[1,5-a][1,3,5] triazin-2-thioxo-4-one with a stronger donor electron ability group.

We note also that we have relatively high coefficients for the atomic charges on atoms C1, C2, C8, N4 and S (qC1, qC2, qC8, qN4 and qS respectively). Thus, high negative charges for C2 and S and high positive charges for C8 and C1 lead to increasing TP inhibitor activity. These charges can be used to explain the physical and electronic molecular properties of the pyrazolo[1,5-a][1,3,5]triazin-2-thioxo-4-ones derivatives contributing to their TP inhibitor potency since the electronic character is directly related to the electron distribution of the drug at the active site⁵⁷.

We used the leave-one-out (LOO) technique to test the validity of the predictive power our model, which is validated by the calculation of the following statistical parameters:

- (i) PRESS (= predicted residual sum of squares) is a good approximation of the real predictive error of the models. It is thus an important cross-validation parameter.
- (ii) SSY (= sum of squares deviation). To have a dependable QSAR model, PRESS/SSY should be smaller than 0.4⁵⁸.
- (iii) S_{PRESS} (predicted squares error) the predictive error of the coefficient of correlation and cross-validated correlation coefficients (r_{adj}^2 and r_{cv}^2).
- (iv) r_{cv}^2 (the overall predictive ability) is a cross-validation correlation coefficient. r_{cv}^2 may vary between 0 and 1. Only QSAR models having ($r_{\text{cv}}^2 > 0.6$) will be considered for validation.
- (i) r_{adj}^2 is a cross-validation correlation coefficient. r_{adj}^2 takes into account the adjustment of R^2 .

Table 7: Cross-validation parameters

Parameter	PRESS	SSY	PRESS/SSY	S _{PRESS}	r_{cv}^2	r_{adj}^2
Value	0.384	16.061	0.023	0.373	0.976	0.952

The results are listed in Table 7. This table shows that PRESS is smaller than SSY. This shows that the model predicts better than chance and can be considered statically significant. The small PRESS value suggests the model predictability. This is further confirmed by the other criteria for the SSY, S_{PRESS}, r_{cv}^2 and r_{adj}^2 parameters. Indeed, the high value of r_{cv}^2 and r_{adj}^2 are essential criteria for the good qualification of the QSAR model.

To go further in the estimation of the predictive power of the developed model, one needs to predict pIC₅₀ values of the investigated pyrazolo[1,5-a][1,3,5]triazin-2-thioxo-4-ones derivatives using this model. Table 8 presents the predicted pIC₅₀ and the measured ones²¹, where a close agreement between both sets of data is observed. We plot in Figure 3 the linear regression of predicted versus experimental values of the biological activity of the pyrazolo[1,5-a][1,3,5] triazin-2-thioxo-4-ones derivatives. A linear regression is found with $R^2 = 0.976$. We searched also for any systematic error in developing the QSAR model. We plotted hence the residuals of predicted values of the biological activity pIC₅₀ against the experimental values (Figure 3). Positive and negative residuals are randomly distributed. Thus, the propagation of the residuals on both sides of zero indicates that no systemic error exists⁵⁹. Therefore, our model can be successfully applied to predict the TP inhibitory activity of this class of molecules.

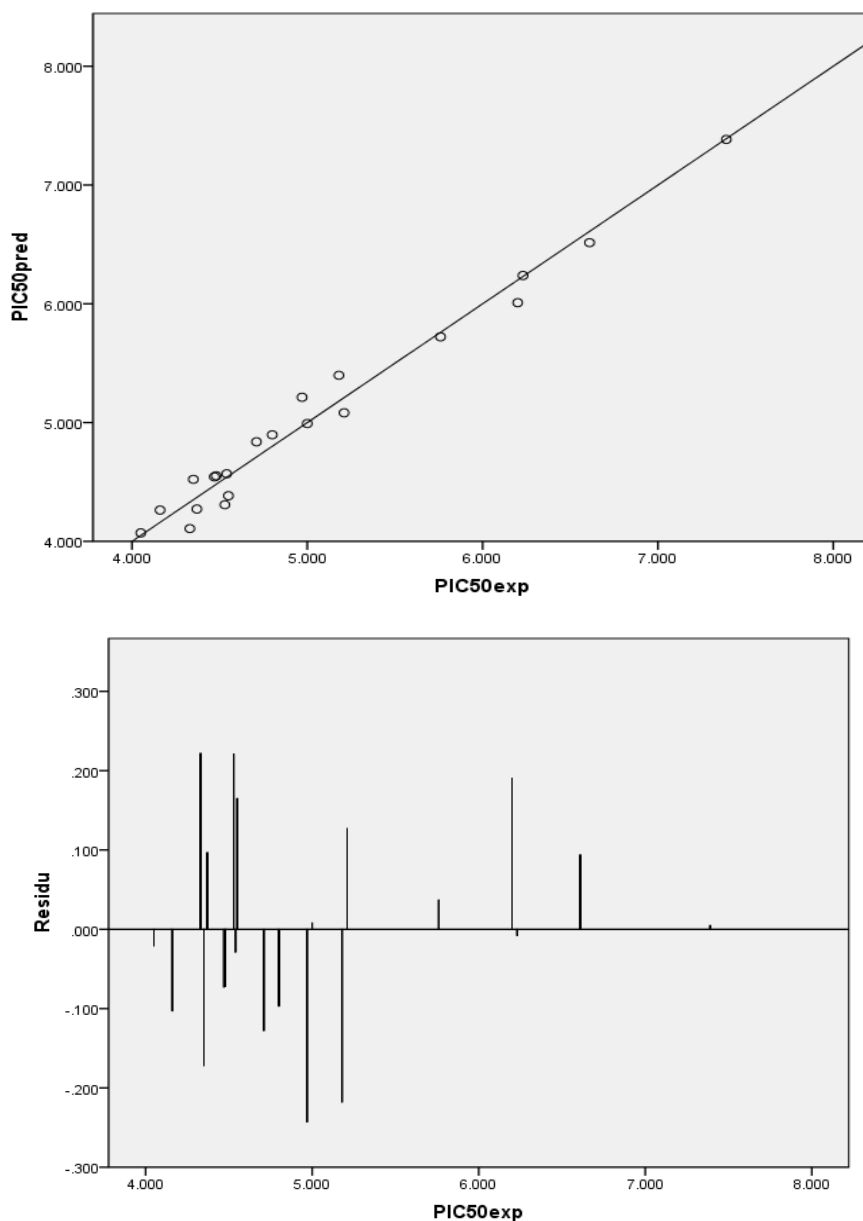


Figure 3: Upper trace: Predicted pIC_{50} versus experimental TP inhibition of pyrazolo[1,5-a][1,3,5]triazin-2-thioxo-4-ones derivatives of interest. Lower trace: Plot of the residual values against the experimentally observed (pIC_{50}).

Table 8: Measured ($pIC_{50 \text{ exp.}}^a$) versus predicted ($pIC_{50 \text{ pred.}}$) activities of pyrazolo[1,5-a][1,3,5]triazin-2-thioxo-4-ones derivatives. We give also the residuals of predicted values of the biological activity pIC_{50} .

Compound	$pIC_{50 \text{ exp.}}^a$	$pIC_{50 \text{ pred.}}$	Residual
1	4.16	4.263	-0.103
2	4.53	4.308	0.221
3	4.48	4.552	-0.072
4	4.37	4.272	0.097

5	4.47	4.543	-0.073
6	5.00	4.992	0.008
7	4.71	4.838	-0.128
8	5.18	5.398	-0.218
9	4.54	4.569	-0.029
10	4.33	4.107	0.222
11	5.21	5.082	0.127
12	4.05	4.071	-0.021
13	4.55	4.384	0.165
14	4.35	4.522	-0.172
15	4.97	5.213	-0.243
16	6.20	6.009	0.190
17	6.61	6.515	0.094
18	5.76	5.722	0.037
19	4.80	4.897	-0.097
20	6.23	6.238	-0.008
21	7.39	7.384	0.005

a. Ref. ²².

VII. Conclusion

After benchmarks we validated the use of B3LYP DFT to predict the structure and the vibrational spectra of a series of twenty-one pyrazolo[1,5-a][1,3,5] triazin-2-thioxo-4-one derivatives. These compounds have a TP inhibitory activity. We found quantitative effects of the molecular structure of the compounds on their TP inhibitory activity. A QSAR model is predicted. It allows establishing quantitative relationships between their physiochemical/quantum properties and their biological activities. Strong correlation between experimental and predicted pIC₅₀ values was obtained, asserting on the high predictive ability of the developed QSAR model. In sum, this model can be successfully applied to predict the TP inhibitory activity of these classes of molecules. As a perspective, data from in-silico docking for the derivatives against TP can be computed. This allows to go further in the evaluation of the inhibitory activity of these compounds and to be ranked based on their binding energies.

References

- [1] R. K. Robins, G. R. Revankar, D. E. O'Brien, R. H. Springer, T. Novinson, A. Albert, K. Senga, J. P. Miller, D. G. Streeter, *J. Heterocycl. Chem.* **1985**, 22, 601-634.
- [2] S. Y. K. Tam, J. S. Hwang, L. H. F.G. De, R. S. Klein, J. J. Fox, *J. Heterocycl. Chem.* **1976**, 13, 1305
- [3] J. N. Vishwakarma, M. Mofizuddin, H. Ila, H. Junjappa, *J. Heterocycl. Chem.* **1988**, 25, 1387.
- [4] E. Fischer, J. Kreutzmann, G. Rembarz, S. Rosenthal, *Pharmazie* **1976**, 31, 546.
- [5] K. Bokri, M. L. Efrat, A. Ben Akacha, *Heterocyclic Letters* **2015**, 5, 679-685.
- [6] T. J. Guzi, K. Paruch, Schering Corporation, USA, **2005**, 45.
- [7] S. Broxer, M. Fitzgerald, C. Sfougataki, J. Defreese, E. Barlow, G. Powers, M. Peddicord, B.N. Su, Y. Tai-Yuen, C. Pathirana, herbine, *J. Org. Process Res. Dev.* **2011**, 15, 343–352.
- [8] D. Zuev, R. Mattson, H. Huang, G. Mattson, L. Zueva, J. Nielsen, E. Kozlowski, X. Huang, D. Wua, G. Gao, N. Lodge, J. Bronson, J. Macor, *Bioorg. Med. Chem. Lett.* **2011**, 21, 2484–2488.
- [9] F. P. Lin Lim, A. V. Dolzhenko. *Eur. J. Med. Chem.* **2014**, 85, 371-390.
- [10] T. Saito, T. Obitsu, C. Minamoto, T. Sugiura, N. Matsumura, S. Ueno, A. Kishi, S. Katsumata, H. Nakai, M. Toda, *Bioorg. Med. Chem.* **2011**, 19, 5955–5966.
- [11] K. Senga, D. E. O'Brien, M. B. Scholten, T. Novinson, J. P. Miller, R. K. Robins, *J. Med. Chem.* **1982**, 25, 243-249.
- [12] K. S. Gudmundsson, B. A. Johns, J. Weatherhead, *J. Bioorg. Med. Chem. Lett.* **2009**, 19, 5689–5692.
- [13] A. V. Dolzhenko, A. V. Dolzhenko, W. K. Chui, *Heterocycles*, **2008**, 75, 1575-1622.
- [14] A. Gescher, M. F. G. Stevens, C. P. Turnbull, *J. Chem. Soc., Perkin Trans.* **1977**, 1 103.
- [15] M. R. H. Elmoghayar, E. A. Ghali, M. M. M. Ramiz, M. H. Elnagdi, *Liebigs Ann. Chem.*, **1985**.
- [16] C. K. Chu, J. Suh, *Nucleic Acid Chem.*, **1991**, 4, 19.
- [17] S. A. A. El Bialya, M. A. Gouda, *J. Heterocycl. Chem.*, **2011**, 48, 1280-1286.
- [18] T. Lübbers, P. Angehrn, H. Gmünder, S. Herzig, J. Kulhanek, *Bioorg. Med. Chem. Lett.* **2000**, 10, 821-826.
- [19] A. J. Duplantier, E. L. Bachert, J. B. Cheng, V. L. Cohan, T. H. Jenkinson, K. G. Kraus, M. W. McKechney, J. D. Pillar, J. W. Watson, *J. Med. Chem.*, **2007**, 50, 344–349.

- [20] M. Narayanan, A. J. Peter, *Quantum. Matter.*, **2012**, 1, 53.
- [21] F. Focher, S. Spadari, *Curr. Cancer Drug Targets.*, **2001**, 1, 141-153.
- [22] L. Sun, H. Bera, W. K. Chui, *Eur. J. Med. Chem.*, **2013**, 65, 1.
- [23] L. Sun, J. Li, H. Bera, A. V. Dolzhenko, G. N. C. Chiu, W. K; Chui. *Eur. J. Med. Chem.*, **2013**, 70, 400-410.
- [24] H. Bera, P. k. Ojha, B. J. Tan, L. Sun, A. V. Dolzhenko, W.-K. Chui, G. N. Chee Chiu. *Eur. J. Med. Chem.*, **2014**, 78, 294-303.
- [25] A. El-Shafei, A. A. Fadda, A. M. Khalil, T. A. E. Ameen, F. A. Badria, *Bioorg. Med. Chem.*, **2009**, 17, 5096–5105.
- [26] Y. Q. Zhu, CH. Wu, H. B. Li, X.M. Zou, X. K. Si, F. Z. Hu, H. Z. Yang, *J. Agric. Food Chem.*, **2007**, 55, 1364-1369.
- [27] M. Alloui, S. Belaidi, H. Othmani, N.-E. Jaidane, M. Hochlaf, *Chem. Phys. Lett.*, **2018**, 696, 70–78.
- [28] M. Narayanan, A. J. Peter, *Quantum. Matter.*, **2012**, 1, 53.
- [29] A. M. Helguera, R. D. Combes, M. P. Gonzalez, M. N. Cordeiro, *Curr. Top. Med. Chem.*, **2008**, 8, 1628–1655.
- [30] A.D. Becke, *J. Chem. Phys.*, **1993**, 98, 5648–5652.
- [31] C. Moller, M. S. Plesset, *Phys. Rev.*, **1934**, 46, 618.
- [32] M.J. Frisch et al., *Gaussian 09, Revision E. 01*, 2009, Gaussian. Inc., Wallingford CT.
- [33] R. Ditchfield, W.J. Hehre, J.A. Pople, *J. Chem. Phys.*, **1971**, 54, 724–728.
- [34] T.H. Dunning Jr, *J. Chem. Phys.*, **1989**, 90, 1007.
- [35] A. E. Reed, L. A. Curtiss, F. Weinhold, *Chem. Rev.*, **1988**, 88, 899–926.
- [36] HyperChem (Molecular Modeling System) Hypercube, Inc., 1115NW, Gainesville, FL 32601, USA, **2008**.
- [37] A. K. Ghose, G. M. Crippen, *J. Chem. Inf. Comp. Sci.*, **1987**, 27, 21.
- [38] K. J. Miller, *J. Am. Chem. Soc.*, **1990**, 112, 8533.
- [39] A. Gavezzotti, *J. Am. Chem. Soc.*, **1983**, 105, 5220.
- [40] N. Bodor, Z. Gabanyi, C. K. Wong, *J. Am. Chem. Soc.*, **1989**, 111, 3783.

- [41] V. N. Viswanadhan, A. K. Ghose, G. R. Revankar, R. K. Robins, *J. Chem. Inf. Comp. Sci.*, **1989**, 29, 163.
- [42] SPSS software packages, SPSS Inc., 444 North Michigan Avenue, Suite 3000, Chicago, Illinois, 60611, USA.
- [43] P. Onkar, S. Leena, N. Kumar, *J At Mol Sci.*, **2010**,1, 201.
- [44] K. S. Rajesh, V. Narayan, *J. Chem. Pharm. Res.*, **2012**, 4, 3287.
- [45] M. L. Laury, M. J. Carlson, A. K. Wilson, *J. Comput. Chem.*, **2012**, 33, 2380–2387.
- [46] P. Lalitha, S. Sivakamasundari, *Orient. J. Chem.*, **2010**, 26, 135.
- [47] Y. Madhu, *Bioinformation.*, **2011**, 7, 388.
- [48] J. Wang, X. Q. Xie, T. Hou, X. Xu, *Fast J. Phys. Chem.*, **2007**, A 24, 4443.
- [49] P. Pankaj, Ch. R. Kapupara, A. S. Matholiya, A. S. Dedakiya, R. D. Tusharbindu, *Inter. Int. Bull. Drug. Res.*, **2011**, 1, 1.
- [50] N. I. Zhokhova, I. I. Baskin, V. A. Palyulin, A. N. Zefirov, N. S. Zefirov, *Russ. Chem. B+*, **2003**, 52, 1061.
- [51] L.B. Kier, Academic Press, New York, NY, USA, **1981**.
- [52] H. Pajouhesh, G. R. Lenz, *Neurotherapeutics*, **2005**, 2, 541.
- [53] E.H. Kerns, L. Di, *Optimization Academic Press, NY, USA.*, **2008**, 43.
- [54] C. A. Lipinski, F. Lombardo, B. W. Dominy, P. Feeny, *J. Adv. Drug Deliv. Rev.*, **1997**, 23, 3-25.
- [55] J. Devore, R. Peck, West Publ. Co, New York **1994**.
- [56] K. J. Sanmati, J. Rahul, S. Lokesh, K. Y. Arvind, *J. Chem. Pharm. Res.*, **2012**, 4, 3215.
- [57] M. Karelson, John Wiley & Sons, New York **2000**.
- [58] S. O. Podunavac-Kuzmanović, D. D. Cvetković, D. J. Barna, *Int. J. Mol. Sci.*, **2009**, 10, 1670.
- [59] M. Jalali-Heravi, A. Kyani, *J. Chem. Inf. Comput. Sci.*, **2004**, 44, 1328.

Graphical abstract

